FATIGUE LIFE PREDICTION OF BRIDGES UNDER EXTREME LOADING

Kamal KARUNANANDA*, Mitao OHGA*, Ranjith DISSANAYAKE**, Kazuhiro TANIWAKI***
Department of Civil and Environmental Engineering, Ehime University, Matsuyama, Japan*
Department of Civil Engineering, University of Peradeniya, Sri Lanka**
Department of Civil and Environmental Engineering, Fukui Institute of Technology, Fukui, Japan***

***ABSTRACT*:** This paper presents a new low cycle fatigue model to predict the life of steel bridges under extreme loading. It consists of Coffin-Mansion strain life relationship and a new damage indicator. The proposed model is verified by comparing model predictions with experimental fatigue results. The proposed model is applied to predict the fatigue life of a bridge member for earthquake loading. The effectiveness of the model is confirmed by comparing the obtained results with the previous Miner's rule based predictions.

KEYWORDS: Low cycle fatigue, extreme loadings, bridges

1. INTRODUCTION

Bridges are generally subjected to high cycle fatigue (HCF) caused by usual traffic loadings (Chen and Liu 1989). Recently, a number of fatigue failures of bridges have been reported that cannot be explained by HCF. Studies on these failures reveal that extreme loading such as earthquakes, typhoons is one of the main reasons for these failures.

In extreme loading situations, bridge members are subjected to high amplitude cyclic loading. Some members may be subjected to stresses in plastic range. The plastic strains may cause low cycle fatigue (LCF) damage in those members and may lead to a reduced service life of bridges (Kondo and Okuya 2007).

In fields such as aircraft and mechanical engineering, the LCF damage has been considered. The commonly used approach of LCF damage prediction is based on Coffin-Mansion strain life relationship (Suresh 1998) with Miner's rule (Miner 1945). However, it has been revealed that Miner's rule does not predict correct results in variable amplitude loadings since it cannot capture the loading sequence effect (Mesmacque et al. 2005 and Siriwardane et al. 2007, 2008). Therefore, the use of the Miner's rule with Coffin-Mansion relationship does not give real life predictions for LCF damages of steel structures. Liu et al. (Liu et al. 2005) have recently proposed and verified a LCF model for accurate life prediction of A36 steel under variable amplitude loading. The model consists of a new damage indicator which was obtained by modifying the Miner's rule considering three multiplications factors such as amplitude change factor, power coefficient for relative strain and partial cycle factor. However, application of this model to other materials, found to be less since these factor determination procedures are lengthy and difficult.

The objective of the paper is to propose a new fatigue model to predict LCF damage of bridges caused by extreme loading. Initially, the proposed model is introduced. Then, verification of the

proposed model is explained. Finally, the proposed model is applied to a bridge member to confirm the applicability and significance of the proposed model.

2. PROPOSED FATIGUE MODEL

This section introduces the new fatigue model to predict the life of steel structures for the LCF damage caused by extreme loading. Total strain is considered as the damage variable in the proposed model. Initially, the details relevant to Coffin-Mansion strain life relationship are discussed. Then, the section clearly describes the new damage indicator.

2.1 Coffin-Mansion strain life relationship

In this study, Coffin-Mansion strain life relationship (Suresh 1998) is utilized in LCF life prediction as shown below.

$$\varepsilon = \frac{\sigma_f^{'}}{E}(2N)^b + \varepsilon_f^{'}(2N)^c \tag{1}$$

where ε is the applied strain amplitude, N is the number of cycles to failure, $\sigma_f^{'}$ is the fatigue strength coefficient, b is the fatigue strength exponent, $\varepsilon_f^{'}$ is the fatigue ductility coefficient, c is the fatigue ductility exponent and E is the elastic modulus of the material. It is shown in Fig. 1 below.

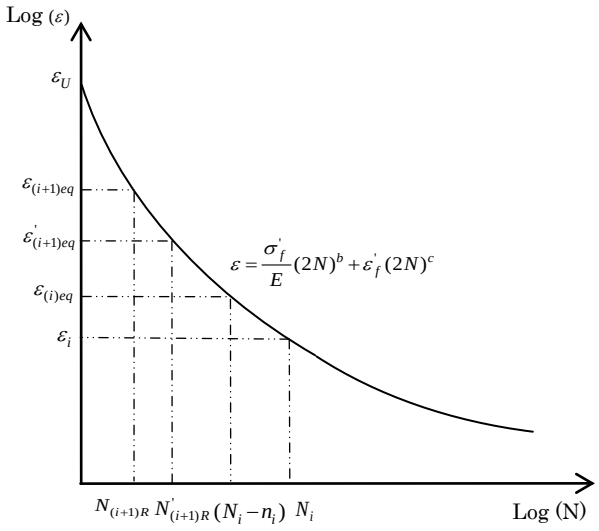

Fig. 1. Coffin-Mansion strain life curve.

These properties are commonly available with most of metallic materials. The ultimate strain of LCF, $(\varepsilon)_U$ which is the total strain corresponding to failure in half reversal (a quarter of a cycle) is obtained from Eq. (1) as,

$$(\varepsilon)_U = \varepsilon_f^{'} \tag{2}$$

2.2 Damage indicator

The hypothesis behind this fatigue law is that if the physical state of damage is the same, then fatigue life depends only on the loading condition. Suppose a member is subjected to a certain strain amplitude $(\varepsilon)_i$ of n_i number of cycles at load level i, N_i is the fatigue life (number of cycles to failure) corresponding to $(\varepsilon)_i$ (Fig. 1). Therefore, the reduced life at the load level i is obtained as $(N_i - n_i)$. The equivalent strain $(\varepsilon)_{(i)eq}$ (Fig. 1), which corresponds to the failure life $(N_i - n_i)$ is named as i^{th} level damage equivalent strain. Hence, the new damage indicator, D_i is stated as,

$$D_i = \frac{(\varepsilon)_{(i)eq} - (\varepsilon)_i}{(\varepsilon)_u - (\varepsilon)_i} \tag{3}$$

Assuming the end of i^{th} loading level, damage D_i has been accumulated (occurred) due to the effect of $(\varepsilon)_{i+1}$ loading cycles, the damage is transformed to load level $i+1$ as below.

$$D_i = \frac{(\varepsilon)_{(i+1)eq}^{'} - (\varepsilon)_{i+1}}{(\varepsilon)_u - (\varepsilon)_{i+1}} \tag{4}$$

Then, $(\varepsilon)_{(i+1)eq}^{'}$ is the damage equivalent strain at loading level $i+1$ and it is calculated as,

$$(\varepsilon)_{(i+1)eq}^{'} = D_i[(\varepsilon)_u - (\varepsilon)_{i+1}] + (\varepsilon)_{i+1} \tag{5}$$

Thus the corresponding equivalent number of cycles to failure $N_{(i+1)R}^{'}$ is obtained from the strain life curve as shown in Fig. 1.

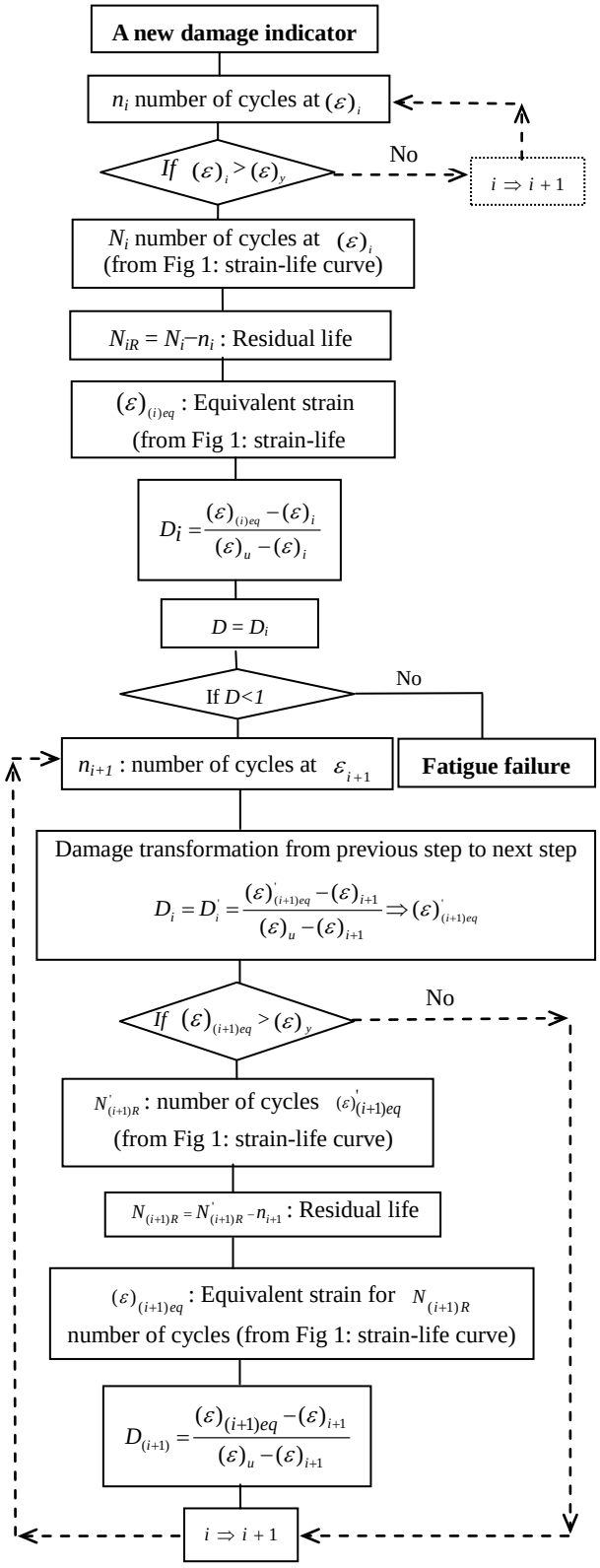

Fig. 2. Flow chart of the proposed damage indicator.

Therefore, the strain $(\varepsilon)_{(i+1)eq}$, which corresponds to the $(\varepsilon)_{i+1}$ is the strain at the level *i+1* and supposing that it is subjected to $n_{(i+1)}$ number of cycles, then the corresponding residual life at load level *i+1*, $N_{(i+1)R}$ is calculated as,

$$N_{(i+1)R} = N'_{(i+1)R} - n_{(i+1)} \tag{6}$$

$N_{(i+1)R}$ at load level *i+1*, is obtained from the strain life curve as shown in Fig. 1.

Then the cumulative damage at the end of load level *i+1* is defined as,

$$D_{(i+1)} = \frac{(\varepsilon)_{(i+1)eq} - (\varepsilon)_{i+1}}{(\varepsilon)_u - (\varepsilon)_{i+1}} \tag{7}$$

At the first cycle the equivalent strain $(\varepsilon)_{(i)eq}$ is equal to $(\varepsilon)_i$ and corresponding damage indicator becomes D_i=0. Similarly at last cycle, the damage indicator becomes D_i=1 when $(\varepsilon)_{(i)eq}$ is equal to $(\varepsilon)_u$. Therefore, the damage indicator is normalized to one (D_i=1) at the fatigue failure of the material. Hence, the above procedure is followed until D_i=1. $(\varepsilon)_y$ is the yield strain of the member material. The proposed damage indicator based algorithm is more clearly explained in the flow chart shown in Fig. 2. Here, the defined fatigue failure is time taken for initiation of crack at the location of maximum stress of the structural member.

3. VERIFICATION OF THE PROPOSED MODEL

The proposed model predicted fatigue lives are compared with experimental LCF lives of a material and Liu et al. model predicted fatigue lives.

3.1 Comparison with experimental fatigue lives

Six fatigue tests (strain controlled and null strain ratio) of P355NL1 steel were carried out with two steps of strain ranges with values of 1% and 0.5% (Pereira et al. 2008). The specimens were tested under two loading sequences which are increasing and decreasing (Fig. 3). Three similar types of specimens were tested under each loading sequence. The tests were carried out in such a way that first block is applied for a specified number of cycles, not

causing material failure. Then, the second block of loading is applied until the failure is observed.

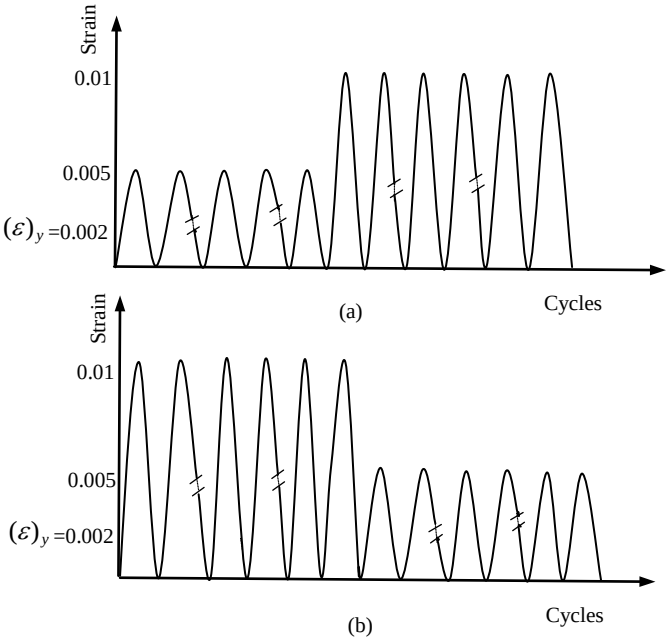

Fig. 3. Applied loading patterns; (a) increasing, (b) decreasing.

Failure number of cycles of these tests was predicted by the proposed model and Miner's rule employed previous model. The obtained results are plotted in Fig. 4. The illustrations of Fig. 4 convince that the proposed model has better correlation with experimental results than Miner's rule employed previous model.

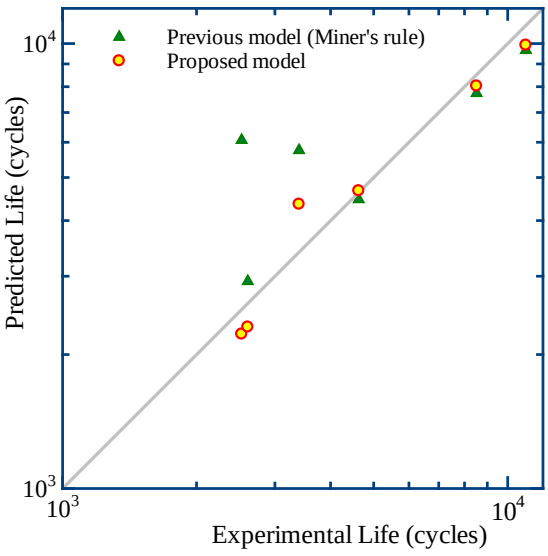

Fig. 4. Comparison of predicted life with experimental life.

3.2 Comparison with precise LCF predicted lives

In this section, this model (Liu et al. 2005) was used to compare the proposed model prediction. The considered material is A36 steel and four repeating block loading patterns were considered as shown in Fig. 5.

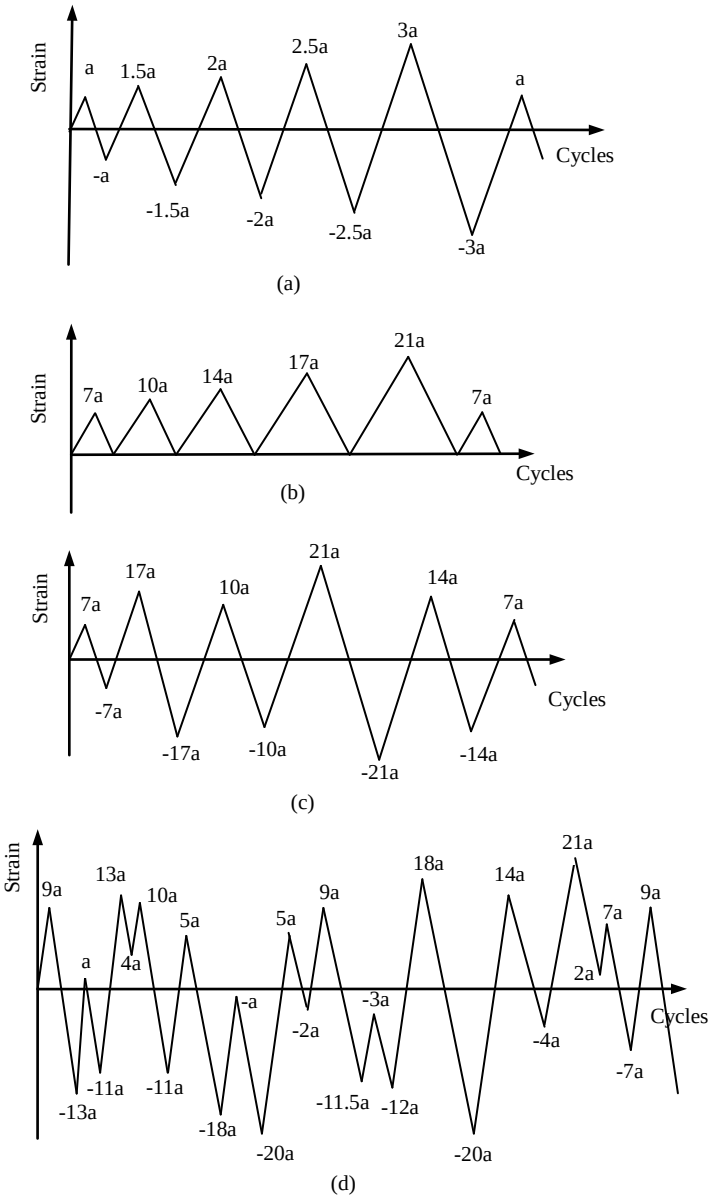

Fig. 5. Loading patterns for A36 steel: (a) pattern I, (b) pattern II, (c) pattern III, (d) pattern IV.

For each pattern, six different strain history blocks were obtained by varying the amplitude of strain (i.e. changing the value "a" of Fig. 5). For pattern i, the values of "a" are 0.015, 0.02, 0.0225, 0.025, 0.0275 and 0.03. For pattern ii, the values of

"a" are 0.002, 0.0025, 0.003, 0.0035, 0.004 and 0.0045. For pattern iii, the values of "a" are 0.0025, 0.003, 0.0035, 0.004, 0.0045, 0.005 and 0.0055. For pattern iv, the values of "a" are 0.0025, 0.003, 0.0035, 0.004, 0.005 and 0.0055. For each history, failure number of cycles was predicted using the proposed model, Liu et al. model as well as Miner's rule employed previous model. The comparisons are given in Fig. 6. These comparisons indicate that the proposed model has better correlation with Liu et al. model for LCF regime than previous model predictions.

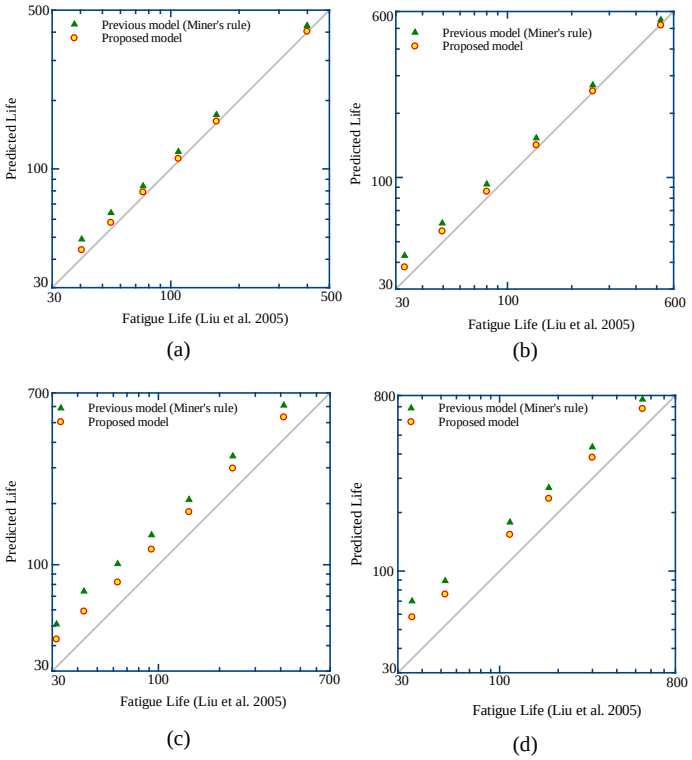

Fig. 6. Comparison of predicted life with the Liu model predicted life for: (a) pattern I, (b) pattern II, (c) pattern III, (d) pattern IV.

4. CASE STUDY

Fatigue life estimation of a bridge member is discussed in this section. The evaluations are especially based on secondary stresses and strains, which are generated around the riveted connection of the member due to stress concentration effect of primary stresses caused by earthquake loadings in addition to usual traffic loadings.

4.1 Considered member

One of the bracing members of the longest railway bridges (Fig. 7(a)) in Sri Lanka (Siriwardane et al. 2007 and 2008) is selected for the life estimation. The selected member is shown in Fig. 7(b). Previous time-history analysis of the global structure of this bridge reveals that this member is also the one of highly stressed member for earthquake loadings.

The LCF damage caused by earthquake loading is estimated using the proposed model and Miner's rule based previous model.

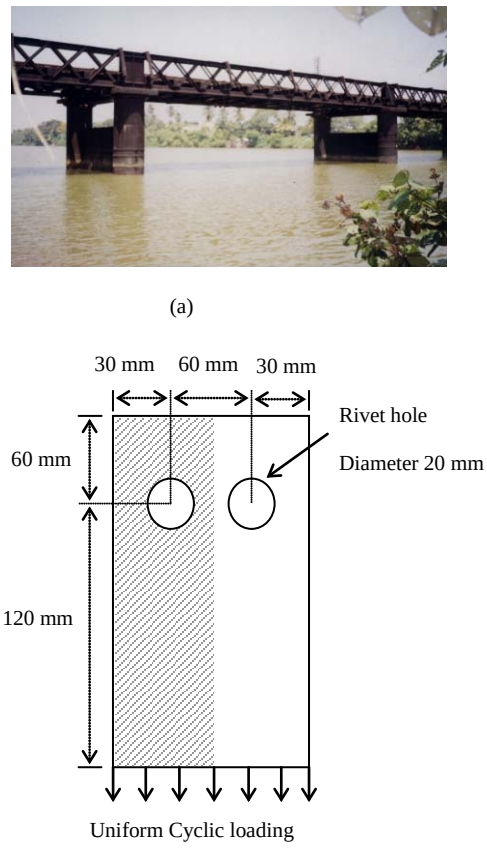

Fig. 7. Considered member: (a) a view of the bridge, (b) geometric details.

The state of strain due to release of contact (tightness) of rivets while all the riveted locations have no clamping force is utilized for fatigue life

estimation.

The clamping force is generally defined as the compressive force in the plates which is induced by the residual tensile force in the rivet. The residual force in the rivets occurs when the rivet get shortened in length due to cooling after a hot rivet is inserted into the hole of plates in order to connect them, and a second head is formed from the protruding shank. Finally clamping force generates a triaxial state of stress in the connected plate (Siriwardane et al. 2007 and 2008). Since this study assumes that the riveted locations have no clamping force (value of clamping force is zero), the connected members are assumed to subject to the biaxial stress state. Therefore, a critical member without rivets can be considered to analyze the biaxial state of stress.

Considering symmetry, one half (hatched area) of the member was considered for FE analysis shown in Fig. 7(b). The nine node isoperimetric shell elements were used for the finite element analysis as shown in Fig. 8(a). The actual air gap restraint conditions were considered in the model to represent unilateral contact between the rivet and the plate.

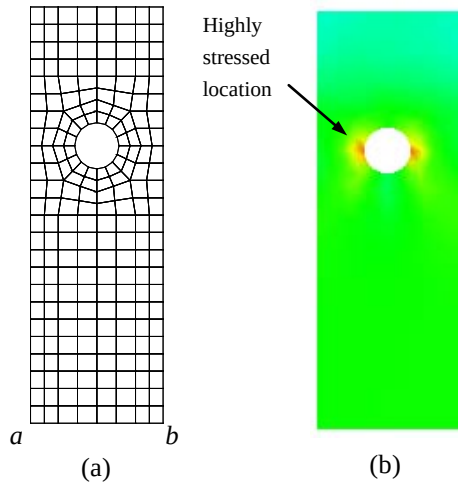

Fig. 8. Maximum von Mises stress (a) FEM mesh, (b) stress distribution.

To make the continuity of the stress field between the global structure and the sub structure, it is required to use any interface between the two structures at every iterative step.

The member is subjected to an earthquake loading (LCF) in addition to usual traffic loadings. Then the elasto-plastic analysis was conducted by applying the primary stress history, which was obtained by time history analysis of global structure under earthquake loading, was applied to the *ab* interface as same as above. The obtained maximum stress contours are shown in Fig. 8(b) and it was decided that state of stress is uniaxial.

The obtained secondary strain variations (Fig. 9) are complex and also irregular shape. These strains should be reduced to a series of equivalent strain cycles at zero mean strain. In order to achieve this objective, initially the famous rainflow cycle counting technique (Dowling and Socie 1982) is used to identify the strain ranges and sequences of closed strain cycles. Then modified Goodman relation is used to transfer these counted cycles to mean strain zero stabilized cycles.

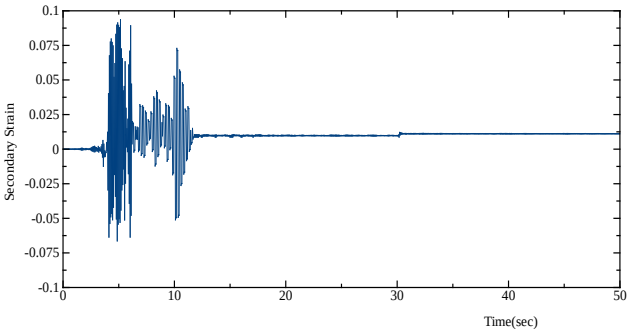

Fig. 9. Secondary strain history of the highly stressed location.

4.2 Strain-life curve

Fatigue properties of the considered bridge member (σ_f', b, ε_f', c and E as shown in Fig. 1) are obtained as 986.5 MPa, -0.11, 0.95, -0.64, and 203

GPa, respectively. From these properties, the corresponding Coffin-Mansion strain life curve for the bridge material was obtained.

4.3 Fatigue life estimation

The damage due to usual traffic loads (HCF) is evaluated by using previously proposed HCF model (Siriwardane et al. 2007). The earthquake induced LCF damage was evaluated using the proposed model as shown in the flow chart (Fig. 2). After the earthquake, the damage due to traffic loads is evaluated using the same HCF model. Further, Miner's rule based previous model was also used to compare the proposed model results.

The fatigue life was estimated when the damage indicator reaches to the unity. Earthquake was considered to occur at different times in the bridge life. The damage values for different earthquake occurrences were obtained as shown in Fig. 10. The fatigue life of the member was estimated as given in Table 1.

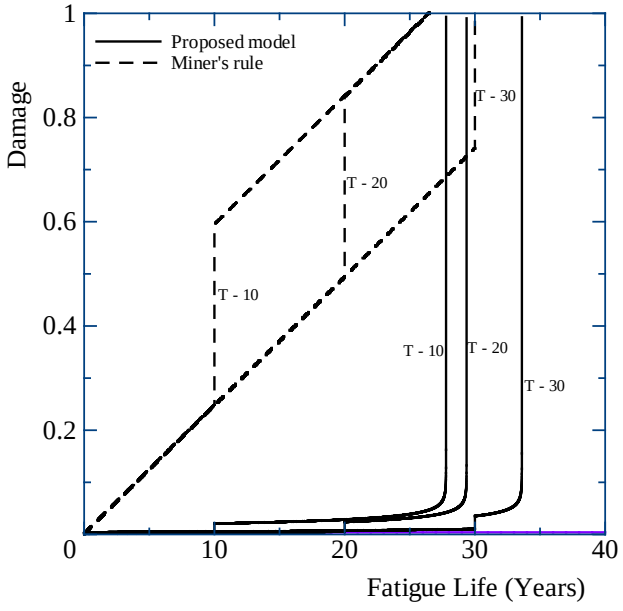

Fig. 10: Damage curves for different stages of bridge life.

An instantaneous increment of damage can be seen when the earthquake is occurred in later stages of bridge life. The results show LCF damage by earthquake loading causes an appreciable reduction of bridge life. Percentage reduction of life is higher when the earthquake occurs at the beginning of the bridge life compared to earthquakes occurring in later times.

Comparison of fatigue life reveals that the proposed model predictions deviate from the previous model predictions. The reduction of service life is constant irrespective of time of earthquake occurrence for previous Miner's rule employed model. The observations of the case study confirm the importance of accurate LCF model to estimate the fatigue life of existing members.

Table1 Comparison of fatigue life

Time of earthquake* (years)	Fatigue life (years)	
	Previous model (Miner's rule)	Proposed model
5	26.5	27.9
10	26.5	27.8
20	26.5	29.4
30	30.0	33.6
Without earthquake	41.0	60.0

*: After construction

5. CONCLUSIONS

A new fatigue model for the LCF damage was proposed for uniaxial stress state. A verification of the model was conducted by comparing the estimated fatigue life with experimental life under variable amplitude loading for one material. Further, the model was verified with a previously proposed LCF model. The proposed fatigue model was further utilized to predict the fatigue life of a bridge member. It was shown that the proposed fatigue model gives a

realistic fatigue life for the LCF damage in variable amplitude loading situation where detailed stress histories are known.

REFERENCES

Chen, W.F. and Lui, E.M., 1987. *Handbook of Structural Engineering*, CRC Press, New York, USA.

Dowling, S.D. and Socie, D.F., 1982, Simple rainflow counting algorithms, *International Journal of Fatigue*, 4(1):31-40.

Kondo, Y. and Okuya, K., 2007. The effect of seismic loading on the fatigue strength of welded joints, *Material Science and Engineering A*, 468-470:223-229.

Liu W., Liang Z. and Lee G., 2005. Low cycle bending fatigue of steel bars under random excitation. Part II: design considerations, *Journal of Structural Engineering*, 131(6):919-923.

Mesmacque, G., Garcia, S., Amrouche, A. and Rubio-Gonzalez, C., 2005. Sequential law in multiaxial fatigue, a new damage indicator, *International Journal of Fatigue*, 27(4):461-467.

Miner, M.A., 1945. Cumulative damage in fatigue. *Journal of Applied Mechanics*, 12:159-64.

Pereira, H.F.S.G., de Jesus, A.M.P., Fernandes, A.A. and Ribeiro, A.S, 2008. Analysis of fatigue damage under block loading in a low carbon steel, *Strain*, 2008; 44(6):429-439.

Siriwardane, S.C., Ohga, M., Dissanayake, R. and Taniwaki K., 2007. Different approaches for remaining fatigue life estimation of critical members in railway bridges, *International Journal of Steel Structures*, 7(4):263-276.

Siriwardane, S., Ohga, M., Dissanayake, R. and Taniwaki, K., 2008. Application of new damage indicator-based sequential law for remaining fatigue life estimation of railway bridges. *Journal of Constructional Steel Research*, 64(2):228-237.

Suresh, S., 1998. *Fatigue of Materials*. UK: Cambridge University Press; Cambridge. UK.